Int. J. Electrochem. Sci., 17 **(2022)** Article ID: 220654, doi: 10.20964/2022.06.68

International Journal of
ELECTROCHEMICAL
SCIENCE
www.electrochemsci.org

Electrochemical Sensor for Detection of Hydrogen Peroxide Based on Cu-doped ZIF-8 material modified with Chitosan and Cytochrome *C*

Hui Yao[1,*], *Wan-ting Zhang*[1], *Ting-yu Yan*[1,2], *Xiao-qin Li*[1], *and Xiao-feng Wang*[1,*]

[1] College of Science, Shenyang University of Chemical Technology, 11# Street Shenyang Economic & Technology Development Area, Shenyang 110142,, P R China
[2] Dalian University of Finance and Economics, Danlian 116620, P R China
[*]E-mail: yaohui_syuct@163.com

Received: 25 June 2021 / *Accepted:* 17 April 2022 / *Published:* 7 May 2022

Metal-Organic Frameworks (MOFs) are promising materials in electrochemical sensor. Herein, Cu-doped zeolitic imidazolate framework (ZIF) was synthesized by hydrothermal method. The prepared composite was characterized by XRD, FTIR and SEM. Then the material was modified onto the surface of glass carbon electrode (GCE) with chitosan(CHIT) and Cytochrome *C*(cyt *c*). The modified electrode showed good electrochemical activity toward the reduction of hydrogen peroxide (H_2O_2). Under optimized conditions, the linear response of the sensor to H_2O_2 ranges from 10～5200 μM, with a detection limit of 3.7 μM (S/N=3). Finally, the sensor was successfully applied to determine H_2O_2 in water samples. Thus, the Cu-doped ZIF material has great potential for applications in electrochemical sensors.

Keywords: MOF, Cu-doped ZIF, modified electrode, hydrogen peroxide

1. INTRODUCTION

The development of nanomaterials provide promising application of sensor. Owing to their special characteristic, many nanomaterials have been reported to fabricate electrochemical sensors in the last few years. Such as metal-based nanoparticles, mesoporous silica nanomaterials and graphite-based which including graphite oxide, graphene, graphene oxide, carbon nanotubes and so on[1,2].

Recently, more and more researchers focus on a new nanomaterial which is Metal-Organic Frameworks (MOFs)[3-6]. MOFs are constructed by connectivity of metal ions and multidentate organic building blocks[7]. Owing to high surface area, tunable pore size, thermal stability and well-defined configuration, MOFs have shown great potential for applications such as gas storage, sensors, catalysis

and electrochemistry[8-13]. Recently, several researchers have begun to explore the potential of MOFs as electrochemical sensors[14]. For example, Wu et al have been developed a sensor based on ZIF-67(Co) MOF as enzymatic mimics to detect concentration of H_2O_2[15]. Wang et al synthesized green octahedral crystals MIL-101(Cr) to detect Pb^{2+} at the trace level by differential pulse anodic stripping voltammetry (DPASV)[16]. However, MOFs materials are still limited in electrochemical applications due to their substantially weaker material properties such as electronic conductivity and electrocatalytic ability[17]. As a result, composites based on MOFs have been considered.

Zeolitic imidazolate frameworks (ZIFs) are a new subclass of crystalline porous metal-organic frameworks (MOFs). ZIF-8 is one of the most studied materials[18], which consists of a Zn source and 2-methylimidazole, and it has sodalite topology structure with an average cage diameter of about 11.6 Å that are accessible through small apertures with a diameter of 3.4 Å[19]. Some reports have indicated that the redox processes can occur in the metal ions and the organic linkers, which is a potential candidate for electrocatalysis and sensing[20]. Doping metal ions based on MOFs displays excellent performance of catalytic in different fields, some reports about that have been published. For example, Yang et al doped copper into ZIF-67 to enhance gas uptake capacity and visible-light-driven photocatalytic degradation of organic dye[21]. Schejn et al doped Cu^{2+} on the ZIF-8 framework to catalyze for cycloadditions and condensation reaction[22]. Zhu et al doped metal ions (Cu^{2+} , Cd^{2+} , or Fe^{2+}) into a gyroidal MOF STU-1, and the doped metal STU-1s improved the performances in adsorption and water stability[23].

In this paper, Cu-doped ZIF-8 nanomaterials was prepared to construct H_2O_2 electrochemical sensor. The detection of H_2O_2 is of great importance in the field of food, biology, industry and medicine. Various methods for the detection of H_2O_2 have been studied, including chemiluminescence [24], fluorescence [25] and electrochemistry [26,27]. Among these methods, electrochemistry technique is especially promising way to detect H_2O_2, due to its simplicity, high sensitivity, low-cost and selectivity[28]. Herein, Cu-doped ZIF-8 materials was hoped to exhibited a good electrocatalysis toward H_2O_2.

2. EXPERIMENTAL

2.1. Chemicals and Reagents

Cytochrome c (cyt c, 95%) and chitosan (CHIT, 200-400mPa.s) were purchased from Aladdin Chemical Co., Ltd (Shanghai, China). NaH_2PO_4•$2H_2O$ (≥99.0%), Na_2HPO_4•$12H_2O$ (≥99.0%), $Cu(NO_3)_2$•$3H_2O$ (≥99.0%), 2-methylimidazole (99.0%) and glutaraldehyde (≥25%) were purchased from Sinopharm Chemical Reagent Co., Ltd. (Shanghai, China). Ethanol (≥99.7%) and methanol (≥99.5%) were purchase from Fu Yu Fine Chemical Co., Ltd. (Tianjin, China). 30% H_2O_2 was purchased from Licheng reagent factory (Shenyang, China). $Zn(NO_3)\cdot 6H_2O$ (≥99.0%) and NH_3•H_2O (≥25%) were purchased from Xinhua reagent factory (Shenyang, China).

The 0.1 M phosphate buffers (PBS) of various pH were prepared by mixing Na_2HPO_4•$12H_2O$ and NaH_2PO_4•$2H_2O$ and adjusted by 0.1 mM NaOH and 0.1 mM HCl solutions. All reagents were of analytical grade and used without further treatment. All solutions were prepared with double-distilled

water. Prior to a series of electrochemical experiments, PBS were purged with highly purified nitrogen for about 20 minutes.

2.2. Apparatus

All electrochemical experiments were carried out in a three-electrode controlled by CHI 660C electrochemical workstation (Shanghai CH Instrument, China). The ZIF-8/cyt c-CHIT/GCE and Cu/ZIF-8/cyt c-CHIT/GCE were used as the working electrode. Reference and auxiliary electrodes were a saturated calomel (SCE) and platinum wire, respectively. Scanning electron micrographs (SEM) image was obtained by scanning electron microscope (Shimadzu JMS-6360LV, Japan). The material was analyzed by X-ray diffraction (XRD) using a D8 Super Speed instrument (Bruker, Germany). FTIR spectra was recorded with a Nicollet 6700 (Thermol Fisher Scientific, America).

2.3. Synthesis of ZIF-8 and Cu-doped ZIF-8

ZIF-8 was prepared based on the literature with some modification [29]. In brief, 2.35g $Zn(NO_3)\cdot 6H_2O$ was added to 100mL $NH_3\cdot H_2O$ and 1.29g 2-methylimidazole was dissolved in 20mL methanol solution. Then, the two solutions were mixed by keeping stirring for 48 hours at room temperature. Next, the mixture was centrifuged three times with methanol. After dried at 80°C overnight, white powder of ZIF-8 was obtained.

1.80g $Cu(NO_3)\cdot 3H_2O$ was dissolved in 30mL ethanol, and then 0.57g ZIF-8 was added under magnetic stirring at room temperature for 2 hours. Then the solution was transferred to Teflon-lined stainless steel autoclave at 200°C for 5 hours. Finally, the product was collected by centrifugation and washed with ethanol and water three times respectively. The material was treated at 600 ℃ for 5 hours in muffle furnace. Black powder of Cu-doped ZIF-8 was obtained.

2.4. Preparation of modified electrodes

GC electrodes were polished with 0.05 μm Al_2O_3 powders on a polishing cloth to obtain a mirror-like surface, and sonicated with nitrate, acetone and double-distilled water for about 3 minutes respectively, and dried with highly purified nitrogen.

2mg Cu-doped ZIF-8 was dispersed into 300μL CHIT solution (0.2 wt% prepared in 0.1 M acetic acid) and sonicated about 50 minutes to get a Cu/ZIF-8-CHIT homogenous solution. Then the Cu/ZIF-8-CHIT solution was mixed with 2mg cyt c for 3 minutes sonication to get a Cu/ZIF-8/cyt c-CHIT homogenous solution. 6.0μL of Cu/ZIF-8/cyt c-CHIT homogenous solution was absorbed by a microinjector and dropped onto the surface of the fresh polished GCE. After dried at room temperature, the modified electrode was incubated for 1 minute in 2% glutaraldehyde solution. Cu/ZIF-8/cyt c-CHIT/GCE was obtained and dried in the air overnight. For comparison, ZIF-8/cyt c-CHIT/GCE was made. The modified electrodes were stored at 4°C in a refrigerator.

3. RESULTS AND DISCUSSION

3.1. Characterization of materials

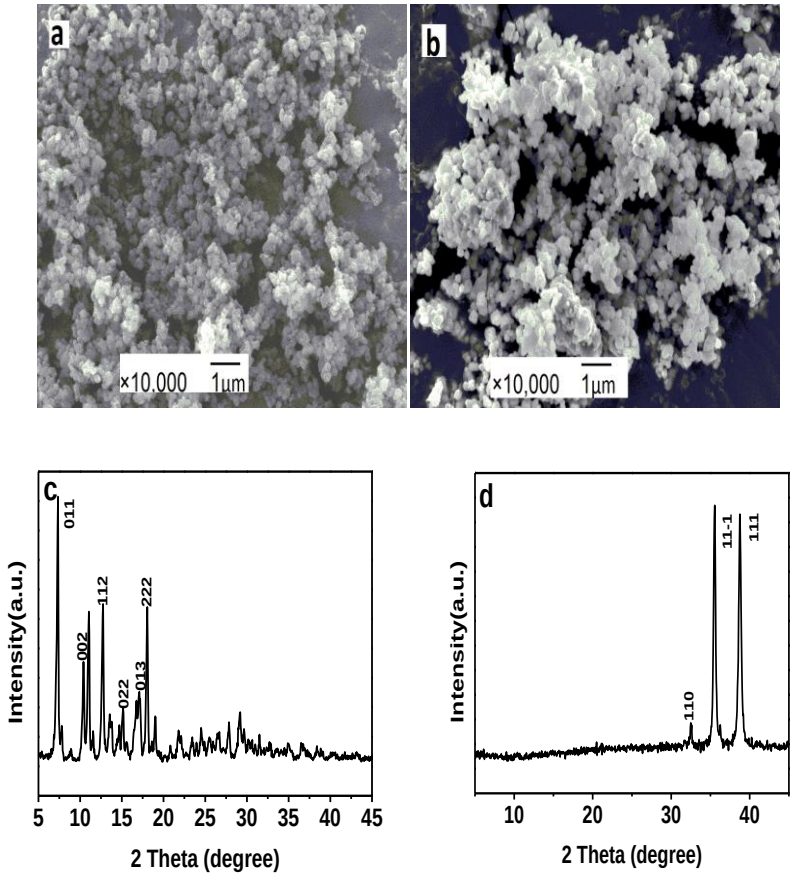

Figure 1. SEM images of (a) ZIF-8 and (b) Cu/ZIF-8 and XRD patterns of (c) ZIF-8 and (d) Cu/ZIF-8.

The morphologies of ZIF-8 and Cu-doped ZIF-8 were characterized by SEM. As shown in Fig. 1 (a) and (b), the particle size of ZIF-8 and Cu-doped ZIF-8 is almost the same and the Cu-doped ZIF-8 displays the same morphology as pure ZIF-8. All materials in SEM images show rather small and monodispersed nanoparticles with a well-defined cubic structure, which is the typical ZIF-8 morphology[22]. The results suggest that the addition of Cu^{2+} ion to the reaction mixture did not affect the framework structure in the ZIF-8 materials.

XRD patterns of ZIF-8 and Cu-doped ZIF-8 were shown in Fig. 1(c) and (d). The characteristic peaks of 011, 002, 112, 022, 013 and 222 are the typical structure of pure ZIF-8(c) crystallinity which in good agreement with previous report[30]. However, the XRD pattern of Cu-doped ZIF-8 is totally different from the XRD pattern of ZIF-8. Fig. 1(d) is the XRD pattern of Cu-doped ZIF-8, and the characteristic peaks of 110,111,11-1 are the typical structure peaks of CuO[31]. The XRD pattern of Cu-doped ZIF-8 can attribute to the mixture of $Cu(NO_3) \cdot 3H_2O$ and ZIF-8 and the surface of ZIF-8 is wrapped by CuO. The results indicate that the surface of ZIF-8 is successfully modified with higher crystallinity level of CuO. Meanwhile, the color of the Cu-doped ZIF-8 changed form white to black with the addition of Cu^{2+} ion into ZIF-8 can also prove that the successful doping of Cu[32].

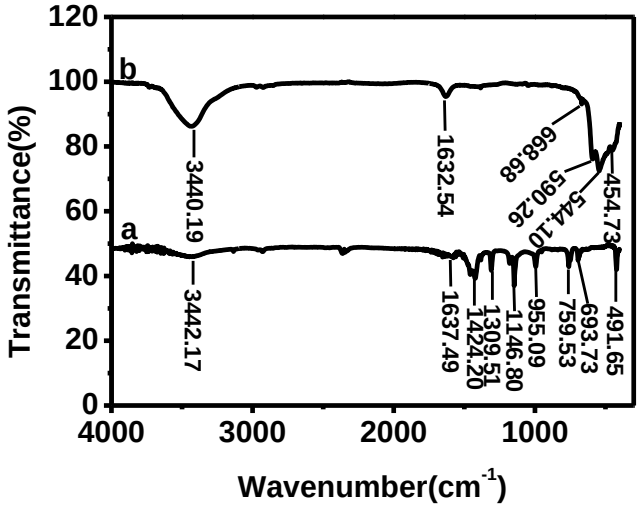

Figure 2. FTIR spectra of ZIF-8 (a) and Cu/ZIF-8(b)

Fig. 2. exhibits the FTIR spectrum of ZIF-8(a) and Cu/ZIF-8(b) samples. As shown, for ZIF-8 (a), the characteristic band of the -OH stretching vibration appeared at about 3442 cm^{-1}, and the peak at about 1637 cm^{-1} corresponded to the stretching vibration of C=O. The absorption bands at 1142 cm^{-1} and 1309 cm^{-1} are assigned to C-H vibrations. The bands in the spectral region of 500～1350 cm^{-1} and 1350～1500 cm^{-1} are the bending and stretching of the imidazole ring respectively. These results confirm the ligand of ZIF-8[33]. For Cu-doped ZIF-8, as shown in Fig. 2(b), the peaks of 3440 cm^{-1} and 1632 cm^{-1} are slightly changed than the peaks of ZIF-8, and the other peaks are different with that of ZIF-8. These results illustrate the presence of the Cu in the composite material.

3.2. Electrochemical sensing performance of Cu/ZIF-8/cyt c-CHIT/GCE

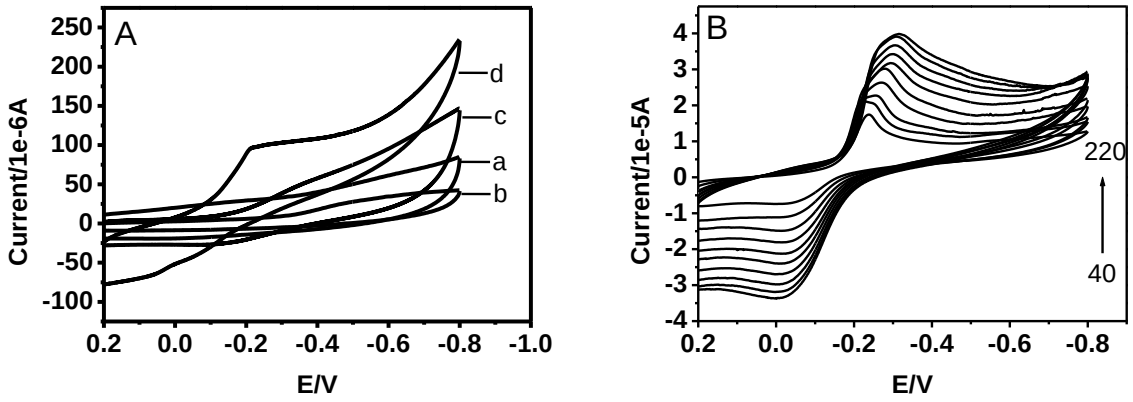

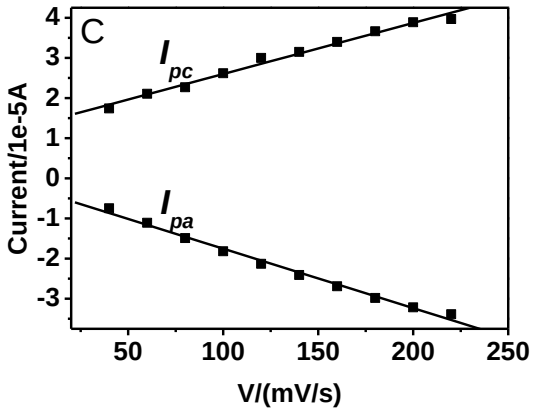

Figure 3. (A) CVs of bare GCE (a), ZIF-8/CHIT/GCE (b), ZIF-8/cyt c-CHIT/GCE (c) and Cu/ZIF-8/cyt c-CHIT/GCE (d), Note: c(PBS)=0.1M, pH=7.0, Scan rate=100 mV/s; (B) CVs of Cu/ZIF-8/cyt c-CHIT/GCE with different scan rates (from inner to outer): 20,40,60,80,100,120,140,160,180,200,220 mV/s; (C) Plots of peak currents versus scan rate.

Cyclic voltammograms of different modified electrodes in 0.1 M (pH 7.0) PBS solution were presented in Fig. 3(A). As shown, there are no redox peaks can be observed at the bare GCE(a) and ZIF-8/CHIT/GCE (b), the redox peak appear at ZIF-8/cyt *c*-CHIT/GCE(c) and Cu/ZIF-8/cyt *c*-CHIT/GCE(d), which should be the effect of cyt *c* transfer electrons to the surface of the electrode. However, the peak currents at Cu/ZIF-8/cyt *c*-CHIT/GCE (d) is higher than ZIF-8/cyt *c*-CHIT/GCE(c). The results prove that Cu/ZIF-8 material can further accelerate the electron transfer reaction of cyt c, and Cu doped in ZIF-8 provide a desirable microenvironment for cyt *c* to transfer electrons to the surface of the electrode. Therefore, Cu/ZIF-8/cyt *c*-CHIT/GCE is selected in the following investigation.

In addition, the electrochemical behavior of Cu/ZIF-8/cyt *c*-CHIT/GCE was further studied by CVs in 0.1 M PBS at pH 7.0 at various potential scan rates, as presented in Fig. 3(B). Both anodic peak currents and cathodic peak currents increase linearly with the potential scan rate in a range from 20 to 200 mV/s. It indicates that the electrode is good of electrochemical reversibility. In Fig. 3(C) the linear regression equation is Ip_a(μA)=-0.27256-0.01481v(mV/s), the correlation coefficient R^2=0.99604(anodic peak), Ip_c(μA)=1.32682+0.01272v(mV/s) and the correlation coefficient R^2=0.99373 (cathodic peak). These results suggest that electrode reaction is the surface controlled process[34].

3.3. Optimization of experimental conditions

The effect of CHIT concentration on electrodes were investigated. The result displayed that the current response increasing shapely from 0.1%～0.2% (wt% of CHIT) and reaching the maximum level at 0.2% (wt%), then decreasing from 0.2%～0.3% (wt%). Therefore 0.2% (wt%) CHIT was chosen in this study.

In order to determine the optimal working potential for H_2O_2 detecting, a plot of chronoamperometric current versus working potential which in the presence of 0.1 mM H_2O_2 was made. The steady state current increased in the range from -0.2 V to -0.3 V and decreased from -0.3 V to -0.4 V, and -0.3 V was selected as the optimized potential.

The effect of pH value on the reduction of H_2O_2 at the Cu/ZIF-8/cyt c-CHIT/GCE was studied. In range from 5 to 9, the current response reach a maximum level at pH 7.0. Thus, PBS at pH 7.0 was chosen to be used for all electrochemical measurements.

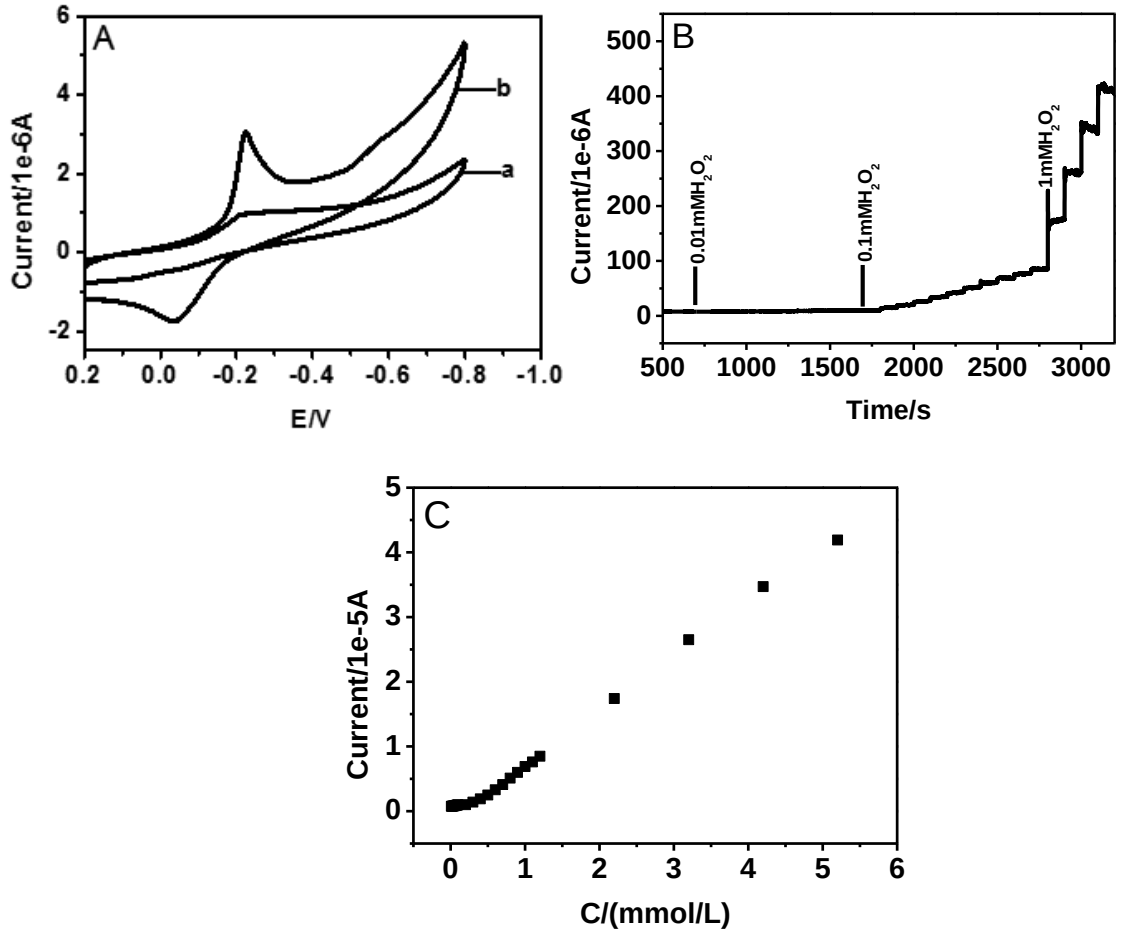

Figure 4. (A) CVs responses of Cu/ZIF-8/cyt c-CHIT/GCE in 0.1 M PBS solution in the absence of H_2O_2 (a) and presence of 0.1 mM H_2O_2 (b). (B) The amperometric response from low H_2O_2 concentration of Cu/ZIF-8/cyt c-CHIT/GCE. (C) Calibration curve for H_2O_2 determination. Note: c (PBS)=0.1 M, pH=7.0, Potential=-0.3 V.

3.4. Electrochemical Detection of H_2O_2

Electrocatalytic behavior of Cu/ZIF-8/cyt c-CHIT/GCE toward H_2O_2 was studied in 0.1 M PBS (pH 7.0) by cyclic voltammetry. As shown in Fig. 4(A), in blank PBS(a), the biosensor only gives the electrochemical behavior of cyt c and a pair of quasi-reversible anodic and cathodic peaks appear in range 0.2 V～-0.8 V. After added 0.1 mM H_2O_2(b), the oxidation peak increasing and the reduction peak

decreasing, which prove that cyt c performs excellent catalysis towards H_2O_2 .

Fig. 4(B) displays the dynamic response of the modified electrode under the optimal experimental conditions. With successive injection of H_2O_2 to the PBS, the reduction current increases stepwise at the Cu/ZIF-8/cyt c-CHIT/GCE. The trace clearly demonstrate the fast response and high sensitivity of the detection to H_2O_2. In Fig. 4(C) the catalytic reduction peak current have a good linear relationship with the concentration of H_2O_2 in the range from 10～5200 μM. The linear regression equation is got as i(μA)=-0.04031+0.81296C(M) and the correlation coefficient R^2=0.99697. The detection limit is 3.7 μM when the signal to noise ratio is 3.

A comparison of various analytical properties of recent amperometric H_2O_2 sensors with the present one is summarized in Table 1.

Table 1. Comparison of the performances of various H_2O_2 biosensors

Electrode	Linear range (μM)	LODs (μM)	Ref.
La (BTC)	5～2670	0.73	35
Cu-hemin MOFs/3D-RGO	10～24400	0.14	36
PCN-222 (Fe)	3～200	1.0	37
MOF(Co/2Fe)	10～100	5.0	38
NC@CuxO	10～500	0.0067	39
ZIF-67/CNFs	2.5～190	0.18	40
Cu/ZIF-8/cyt *c*-CHIT/GCE	10～5200	3.7	This work

3.5. Interference, Reproducibility and stability of Cu/ZIF-8/cyt c- CHIT/GCE

The effect of possible interferences was studied by detecting H_2O_2 under 1 mM H_2O_2 in 0.1 M pH 7.0 PBS. It was founded that diluted 10-fold concentration of tyrosine, tryptophan, glucose, uric acid, histidine, glutamate, ascorbic acid did not interfere with the determination of H_2O_2. From the results, it is concluded that the Cu/ZIF-8/cyt *c*-CHIT/GCE has good selectivity for the determination of H_2O_2.

To test the stability, the sensor was estimated to measure 0.1 mM H_2O_2. After 40 cycles of cyclic voltammetry, the sensor retain 82.9% of the initial current value. Furthermore, in order to evaluate its reproducibility, the same electrode was used for five measurements with the obtained relative standard deviation (RSD) was 7.9%.

3.6. Application of Cu/ZIF-8/cyt c-CHIT/GCE in Real Samples

Table 2. The determination of H_2O_2 in tap water samples.

Sample	Added(mM)	Found(mM)	Recovery(%)	RSD(%, n=3)
1	0.250	0.245	98	1.2
2	0.500	0.493	99	2.7
3	1.000	1.036	104	1.0

In order to verify the feasibility of Cu/ZIF-8/cyt *c*-CHIT/GCE sensor in practical applications, the sensor was used to detect real water samples. The tap water samples were diluted by combining 5:5 volume ratio of phosphate buffer solution (pH 7.0) and tap water before test. 0.25, 0.5 and 1 mM concentrations of H_2O_2 were added to water samples respectively. The results were showed in table 2. The desirable recoveries suggest that the biosensor presents a promising potential application in real samples.

4. CONCLUSIONS

In this work novel enzyme sensors have been designed based on the ZIF-8 and Cu-doped ZIF-8 composite. Experiments have proved that Cu-doped ZIF-8 was of efficient than ZIF-8. In this paper, the Cu/ZIF-8/cyt c-CHIT/GCE sensor showed excellent electrocatalytic ability for the reduction of H_2O_2, the detection limit can reach 3.7 μM and linear range from 10～5200 μM. The sensor could provide a new platform for expanding the application of metal organic frameworks in the fields of electrochemistry sensor.

ACKNOWLEDGEMENT
We gratefully acknowledge the financial support for this project from the Public Welfare Scientific Research Project of Liaoning Province of China (No. 20170008), and the Foundation of Shenyang University of Chemical Technology (No. LJ2020011).

References

1. P. Yáñez-Sedeño, A. González-Cortés, S. Campuzano and J. M. Pingarrón. *Nanomaterials*, 10 (2020) 2556.
2. J. Xu , Y. Wang , S. Hu. *Microchim Acta*, 184 (2017) 1.
3. D. D. Wang, D. Jana, and Y. L. Zhao. *Acc. Chem. Res.,* 53 (2020) 1389.
4. Y. Du, X. Jia, L. Zhong, Y. Jiao, Z. Zhang, Z. Wang, Y. Feng, M. Bilal, J. Cui, S. Jia. *Coord. Chem. Rev.,* 454 (2022) 214327.
5. S. Liang, X.L. Wu, J. Xiong, M.H. Zong, W.Y. Lou, *Coord. Chem. Rev.,* 406 (2020) 213149.

6. Y. Fan, J. Zhang, Y. Shen, B. Zheng, W.N. Zhang, F.W. Huo. *Nano Res.* 14(2021)1.
7. H. R. Moon, D. W. Lim and M. P. Suh. *Chem. Soc. Rev*., 42 (2013) 1807.
8. X. Niu, X. Li, Z. Lyu, J. Pan, S. Ding, X. Ruan. *Chem Commun*., 56 (2020)11338.
9. S. Kempahanumakkagari, K. Vellingiri, A. Deep, E.E. Kwon, N. Bolan, K.H. Kim, *Coord. Chem. Rev.,* 357 (2018) 105.
10. C. Chuang and C. Kung. *Electroanalysis*, 32 (2020) 1885.
11. C. S. Liu, J. Li, H. Pang, *Coord. Chem. Rev.,* 410 (2020) 213222.
12. M. Li, G. Zhang, A. Boakye, H. Chai, L. Qu and X. Zhang. *Front. Bioeng. Biotechnol.*, 9 (2021) 797067.
13. S. M. Feng, X. L. Zhang, D. Y. Shi, Z. Wang, *Front. Chem. Sci. Eng.*, 15 (2021) 221.
14. G. L. Luo , Y. Deng, H. Xie, J. Liu, S. Mi, B. H. Li, G. J. Li, W. Sun. *Int. J. Electrochem. Sci.*, 14 (2019) 2732.
15. Z. Wu, L.P. Sun, Z. Zhou, Q. Li, L.H. Huo, H. Zhao, *Sensors & Actuators: B.,* 276 (2018) 142.
16. Y. J.Wang, K. J. Du, Y. F.Chen, Y. J. Li and X. W. He. *Anal. Methods.*, 8 (2016) 3263.
17. E. C. Zhou, Y. W. Zhang, Y. J. Li, and X. W. He. *Electroanalysis*., 26 (2014) 2526.
18. K. Kida, K. Fujita, T. Shimada, S. Tanaka and Y. Miyake. *Dalton Trans*., 42 (2013) 11128.
19. K. Kida, M. Okita, K. Fujita, S. Tanaka and Y. Miyake. *CrystEngComm*., 15 (2013) 1794.
20. Y. Wang, Y. C. Wu, J. Xie, H. L. Ge and X. Y. Hu. *Analyst*., 138 (2013) 5113.
21. H. Yang, X. W. He, F. Wang, Y. Kang and J. Zhang. *Mater. Chem*., 22 (2012) 21849.
22. A. Schejn, A. Aboulaich, L. Balan, V. Falk, J. Lalevée, G. Medjahdi, L. Aranda, K. Mozet and R. Schneider. *Catal. Sci. Technol*., 5 (2015) 1829.
23. X. W. Zhu, X. P. Zhou and D. Li. *Chem. Commun*., 52 (2016) 6513.
24. Z. H. Wang, F. Liu, X. Teng, C. X. Zhao and C. Lu. *Analyst*., 136 (2011) 4986.
25. Y. F. Huan, Q. Fei, H. Y. Shan, B. J. Wang, H. Xu and G. D. Feng. *Analyst*., 140 (2015) 1655.
26. D. Xu, L. Li, Y. P. Ding and S. Q. Cui. *Anal. Methods*., 7 (2015) 6083.
27. J. Luo, Y. Z. Chen, Q. Ma, R. Liu and X. Y. Liu. *J. Mater. Chem. C*., 2 (2014) 4818.
28. R. R. Jin, L. F. Li, Y. H. Lian, X. F. Xu and F. Zhao. *Anal. Methods*., 4 (2012) 2704.
29. Chizallet C, Lazare S, Bazer-Bachi D, et al. *J. Am. Chem. Soc*., 132 (2010) 12365.
30. N. Nagarjun and A. Dhakshinamoorthy. *New J. Chem.*, 43 (2019) 18702.
31. Y. H. Song, D. Q. Hu, F. F. Liu, S. H. Chen and L. Wang. *Analyst*., 140 (2015) 623.
32. Y. Dai, P. Xing, X. Cui, Z. Lia, and X. Zhang. *Dalton Trans.*, 48 (2019) 16562.
33. H. Hosseini, H. Ahmar, A. Dehghani. *Electrochim. Acta*., 88 (2013) 301.
34. C. Lei, S. Hu, G. Shen and R. Yu, *Talanta*., 59 (2003) 981.
35. Y. Li, Y. Zhong, J. Huang, *Chem. Pap.*, 71 (2017) 913.
36. S. Zhou, L. Jiang, J. Zhang, P. Zhao, M. Yang, D. Huo, X. Luo, C. Shen, C. Hou. *Microchimica Acta,* 188 (2021) 160.
37. M. Aghayan1, A. Mahmoudi1, K. Nazari, S. Dehghanpour, S. Sohrabi, M. R. Sazegar, N. M. Tabrizi. *Journal of Porous Materials* 26 (2019) 1507.
38. H. Yang, R. Yang, P. Zhang, Y. Qin, T. Chen, F. Ye. *Microchim Acta*, 184 (2017) 4629.
39. J. Li, W.L. Xin, Y.X. Dai, G. Shu, X.J. Zhang, R. S. Marks, S. Cosnier, and D. Shan. *Anal. Chem.* 93 (2021) 11066.
40. Y. Fu, J. Dai, Y. Ge, Y. Zhang, H. Ke, W. Zhang, *Molecules* 23 (2018) 2552.